Geophysical Research Letters

RESEARCH LETTER
10.1029/2019GL086810

Special Section:
The Arctic: An AGU Joint Special Collection

AMOC Recovery in a Multicentennial Scenario Using a Coupled Atmosphere-Ocean-Ice Sheet Model

L. Ackermann[1], C. Danek[1], P. Gierz[1], and G. Lohmann[1]

[1]Alfred-Wegener-Institut, Helmholtz-Zentrum für Polar- und Meeresforschung, Bremerhaven, Germany

Abstract We simulate the two Coupled Model Intercomparison Project scenarios RCP4.5 and RCP8.5, to assess the effects of melt-induced fresh water on the Atlantic meridional overturning circulation (AMOC). We use a newly developed climate model with high resolution at the coasts, resolving the complex ocean dynamics. Our results show an AMOC recovery in simulations run with and without an included ice sheet model. We find that the ice sheet adds a strong decadal variability on the freshwater release, resulting in intervals in which it reduces the surface runoff by high accumulation rates. This compensating effect is missing in climate models without dynamic ice sheets. Therefore, we argue to assess those freshwater hosing experiments critically, which aim to parameterize Greenland's freshwater release. We assume the increasing net evaporation over the Atlantic and the resulting increase in ocean salinity, to be the main driver of the AMOC recovery.

Plain Language Summary The Atlantic Ocean circulation is an important factor within the Earth's climate system. Part of this overturning are specific regions in the North Atlantic where water masses get heavier and sink down. It is speculated that huge amounts of fresh water could disturb this process and weaken the circulation. Because of global warming, one source of this fresh water might be melt water from the Greenland ice sheet. Global warming will also lead to stronger precipitation over Greenland. We show in different future scenarios that the Greenland ice sheet is not only melting but also growing in some areas. The amount of melt water that flows into the ocean shows a strong fluctuation. We find that the melting of the Greenland ice sheet will not have a big effect on ocean circulation.

Key Points:
- The Atlantic meridional overturning circulation recovers after a slowdown in CMIP's RCP8.5 scenario
- The Greenland ice sheet acts as a freshwater source and sink, compensating melting by local ice growth and shows little effect on the AMOC
- The interbasin atmospheric freshwater flux is a main driver for the AMOC recovery

Supporting Information:
- Supporting Information S1
- Figure S1
- Figure S2
- Figure S3

Correspondence to:
L. Ackermann,
lars.ackermann@awi.de

Citation:
Ackermann, L., Danek, C., Gierz, P., & Lohmann, G. (2020). AMOC recovery in a multicentennial scenario using a coupled atmosphere-ocean-ice sheet model. *Geophysical Research Letters*, *47*, e2019GL086810. https://doi.org/10.1029/2019GL086810

Received 29 DEC 2019
Accepted 22 JUL 2020
Accepted article online 4 AUG 2020

1. Introduction

The Atlantic meridional overturning circulation (AMOC) plays a crucial role in Earth's climate system. It has been shown that it may be affected by freshwater perturbations and changes in ocean temperature (Bryan, 1986; Clark et al., 2002; Manabe & Stouffer, 1995; Rahmstorf, 2002). Paleoclimate studies have found that its strength can be linked to abrupt climate changes in the past (Broecker et al., 1985; Keigwin et al., 1991; McManus et al., 2004). Examples for these changes are the so-called "Little Ice Age" (Bianchi & McCave, 1999; Broecker, 2000; Thibodeau et al., 2018) or the Last Termination and Heinrich Events (Barker et al., 2009, 2010; Broecker, 1990; Broecker et al., 1988; Knorr & Lohmann, 2007). With respect to global warming, several studies suggest a future slowdown (Gierz et al., 2015; Golledge et al., 2019; Stocker & Schmittner, 1997; Swingedouw & Braconnot, 2007; Weaver et al., 2012) and observations of sea surface temperature (SST), that can be used as a proxy for AMOC strength, already indicate a recent slowdown since the mid-twentieth century (Dima & Lohmann, 2010). However, the extent of the future weakening and the parts of different mechanisms affecting the AMOC are still unclear. One of these mechanisms is the potential future melting of the Greenland ice sheet (GIS), which might lead to the release of huge amounts of fresh water into the northern North Atlantic. Studies by Latif et al. (2000) and Lohmann (2003) suggest a strong atmospheric freshwater export from the Atlantic as an AMOC stabilizing effect in warm climates and those with a weak AMOC, respectively.

Studies for phase five of the Climate Model Intercomparison Project (CMIP5) suggest a further future weakening of the AMOC for different IPCC scenarios. Weaver et al. (2012) analyzed 30 of these models and found an AMOC weakening of 23–30% for the Representative Concentration Pathway (RCP) scenario RCP4.5 and a weakening of 36–44% for the RCP8.5 scenario. While most CMIP5 models deploy land surface and hydraulic models and capture, for example, surface runoff and snow accumulation, they generally do not include

explicit ice sheet models (ISM). Therefore, they lack important feedbacks, such as melt elevation feedbacks and inherent fluxes from ice through calving and basal melting. To compensate for these drawbacks, some studies use ad hoc water hosing without explicitly simulating the location of freshwater release (e.g., Hu et al., 2009, 2011; Jungclaus et al., 2006; Stammer et al., 2011).

Studies with coupled climate ice sheet models have been performed (e.g., Driesschaert et al., 2007; Gierz et al., 2015; Golledge et al., 2019; Lenaerts et al., 2015; Mikolajewicz et al., 2007), but with limitations regarding the resolution, the coupling, or the forcing applied. It has been suggested that the location of freshwater inflow is essential to accurately assess the effect of ice sheet melting on the AMOC (Y. Liu, Hallberg, et al., 2018). While freshwater fluxes from the GIS can affect deep water formation in the Labrador Sea (Yang et al., 2016) and AMOC (Weijer et al., 2012), other studies show only weak interactions between west of Greenland, the Labrador Current, and the Labrador Sea (Eden & Böning, 2002; Schmidt & Send, 2007; H. Wang, Legg, et al., 2018). Böning et al. (2016) suggest that only small amounts of GIS meltwater reach the Labrador Sea with little effect on the AMOC. Danek et al. (2019) find that the resolution in the ocean circulation model matters for the Labrador Sea convection and that such areas can play an important role in realistically simulating the variability in AMOC.

Additionally, to the melting of ice sheets, the melting of sea ice might play a crucial role in a possible future AMOC slowdown (W. Liu, Fedorov, et al., 2019). Here, we want to improve the understanding of effects by GIS melting on the AMOC by identifying the main contributors to a possible future AMOC slowdown and address different feedback mechanisms. For that, we use a multiresolution atmosphere-ocean-ice sheet model with increased resolution in the northern North Atlantic to run different future scenarios.

2. Methods

The model is based on the AWI Earth System Model (AWI-ESM), which consists of the AWI Climate Model (AWI-CM) (Rackow et al., 2018; Sidorenko et al., 2015), but with interactive vegetation and Northern Hemisphere ice sheet. The model comprises the atmosphere model ECHAM6 (Stevens et al., 2013), which is run with the T63L47 setup, that is, a horizontal resolution of 1.85° × 1.85°. The ocean-sea ice model FESOM1.4 (Q. Wang, Danilov, et al., 2014) employs an unstructured grid, allowing for varying resolutions from 20 km around Greenland and in the North Atlantic to around 150 km in the open ocean (CORE2 mesh). Here, the dynamic ice sheet model PISM1.1 (Martin et al., 2011; Winkelmann et al., 2011) is dynamically coupled to the ocean and atmosphere components. The ice sheet model is used for the GIS domain with a resolution of 5 km. The land surface processes are computed by the land surface model JSBACH2.11 (Reick et al., 2013). The model considers the surface runoff toward the coasts, deploying a hydrological discharge model that also includes freshwater fluxes by snowmelt (Hagemann & Dümenil, 1997). However, for areas without infiltration, the whole precipitation is passed to the river runoff, and thus, no snow accumulation can occur. This also applies to glacial areas like Greenland and Antarctica (Hagemann & Gates, 2003). Therefore, in our coupled model setup, the total mass balance from the ice sheet model is added to the surface runoff by the land surface model to account for surface accumulation.

Our model strategy is that we perform experiments with AWI-ESM with and without the interactive ice sheet component. Control simulations are run for both model setups (CTRL, CTRL-ice) for 399 and 408 years, respectively. For those runs, greenhouse gas (GHG) forcing is fixed at an assumed preindustrial level (Figure 1a). Historical runs are performed, starting from the Year 1850 (HIST, HIST-ice), that are forced with historical GHG concentrations, reconstructed from observations. We investigate two different future scenarios following the Representative Concentration Pathway (RCP). These are the RCP4.5 (Clarke et al., 2007; Wise et al., 2009) and the RCP8.5 (Riahi et al., 2007) scenarios, corresponding to atmospheric CO_{2eq} concentrations by the Year 2100 of 581 and 1,231 ppm, respectively. These CO_2 concentrations represent a combined equivalent of all projected anthropogenic forcing, including landuse change and aerosol emissions. To be able to investigate the effects of global warming on the ice sheet, the simulations are prolonged to the Year 2200, fixing the CO_{2eq} concentrations of the Year 2100. Each scenario is simulated with (RCP4.5-ice, RCP8.5-ice) and without interactive GIS (RCP4.5, RCP8.5).

3. Feedback of Ocean and Atmosphere

The global surface average temperature increases from around 13°C to above 16°C in the RCP4.5 scenario and about 19.5°C in the RCP8.5 scenario (Figure 1b). There are no significant differences between the results,

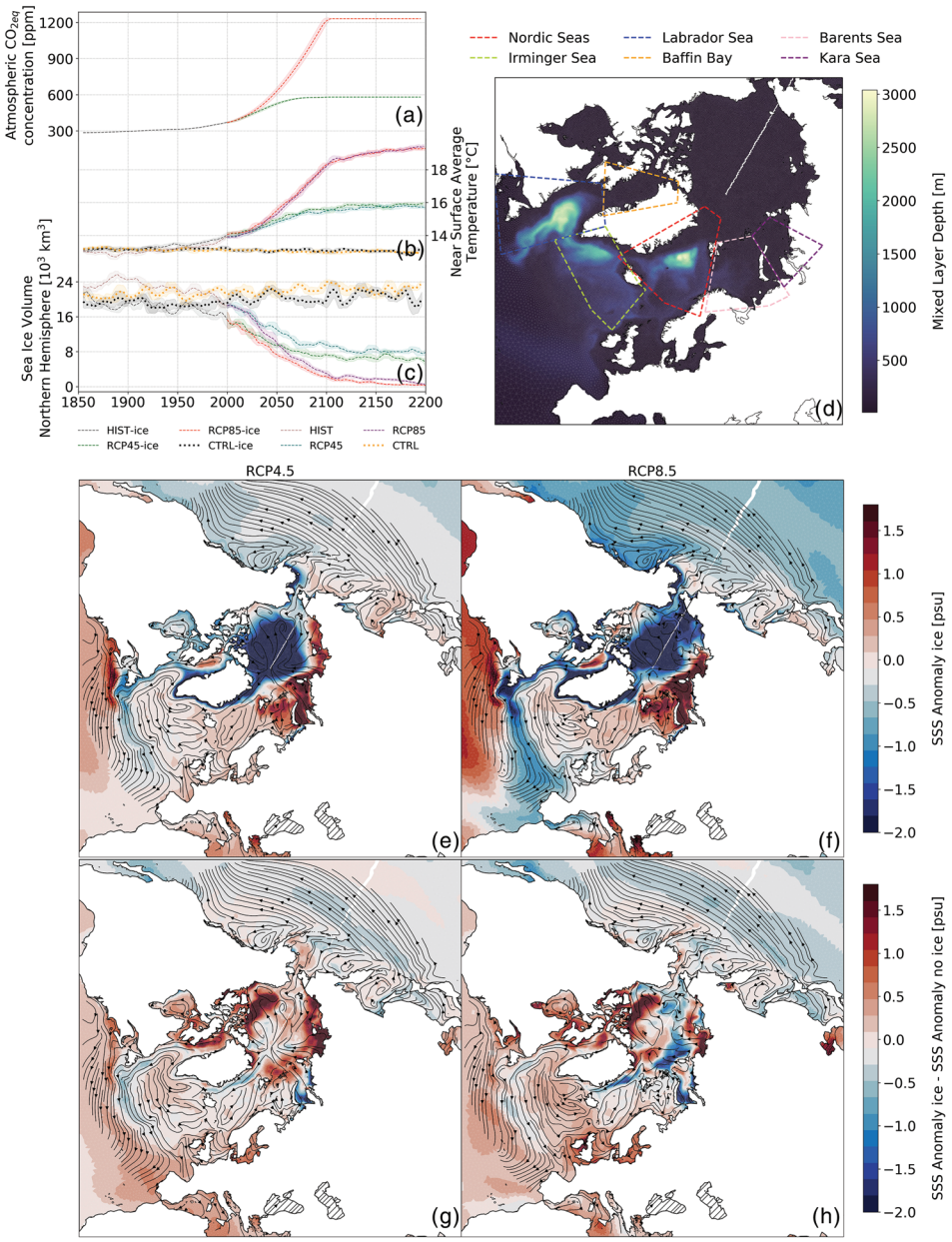

Figure 1. Time series of 11-year mean (a) CO_2 forcing as concentration of CO_2 equivalent in the atmosphere, (b) global near-surface average temperature, (c) sea ice volume in the Northern Hemisphere; shaded areas indicate 1 standard deviation; (d) North Atlantic mixed layer depth with Barents Sea, Baffin Bay, Kara Sea, Labrador Sea, Nordic Seas, Irminger Sea; (e, f) SSS anomaly for the coupled model setup for 2170–2199, (g, h) SSS anomaly difference between coupled and uncoupled model setup for 2170–2199. Arrows indicate surface streamlines.

including the ice sheet and without. Regarding the sea surface salinity (SSS), most areas in the North Atlantic show an increase in SSS (Figures 1e–1h). The anomaly is very pronounced in the Barents Sea, the Kara Sea, and the Baffin Bay, with SSS increasing by around +2 psu. The strongest decrease in P-E occurs over the Atlantic between 10°N and 40°N as well as 10°S and 40°S, reaching values of up to −1 m year^{-1} in the RCP8.5 scenario (Figure 2). An increase in P-E can be seen over Greenland and North Europe and also over the Labrador Sea and the Irminger Sea. This pattern is more distinctive in the RCP8.5 scenario, and differences between the two model results are relatively weak (Figure S1 in the supporting information). The pattern of $P - E < 0$ for the low latitudes and $P - E > 0$ for the high latitudes gets enhanced in both future scenarios, whereas no significant differences between the two model results can be seen.

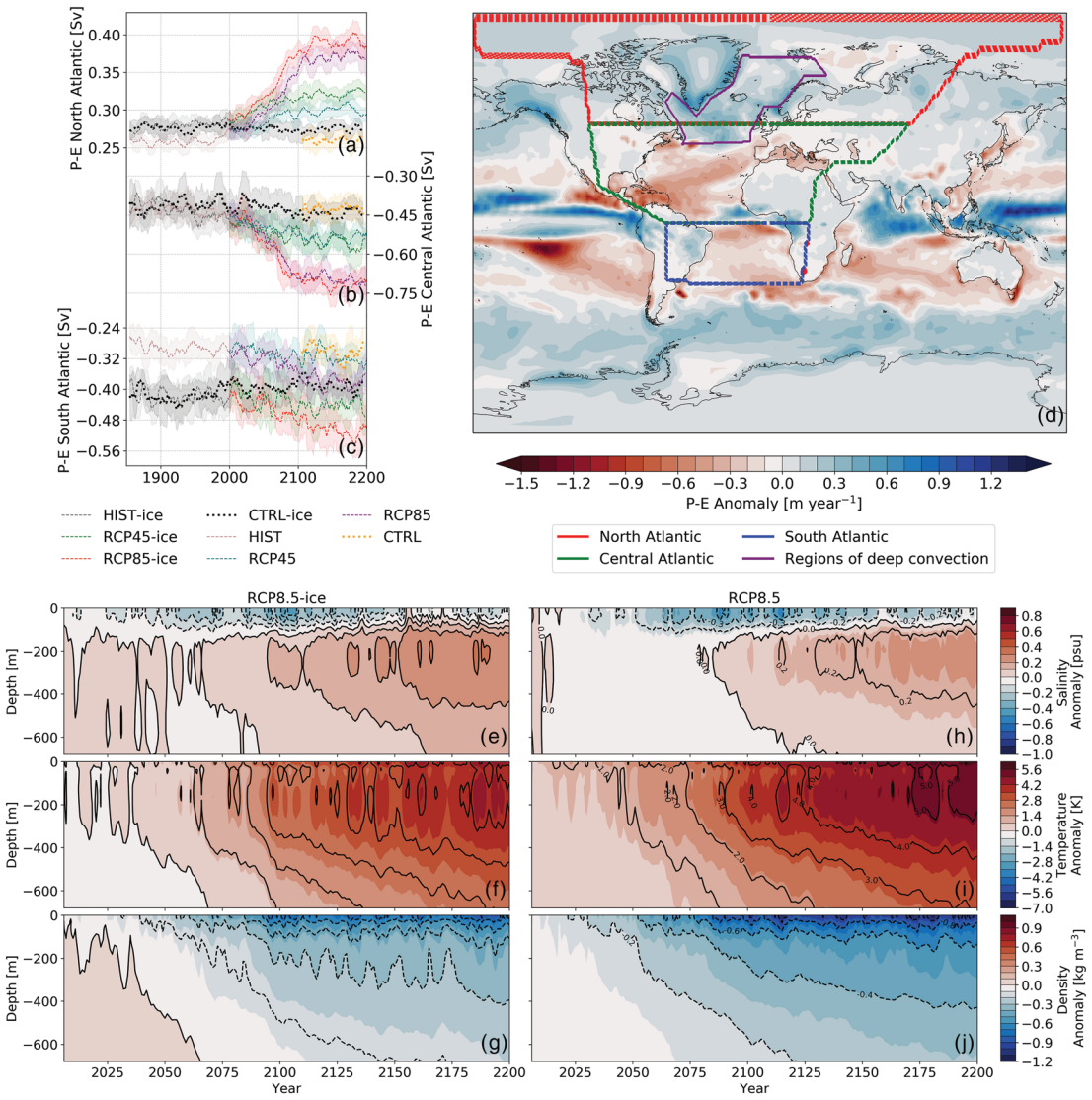

Figure 2. Time series of 11-year mean P-E integrated over the catchment areas of (a) North Atlantic, (b) Central Atlantic, (c) South Atlantic for all scenarios; shaded areas indicate 1 standard deviation; for CTRL only the last 100 years are shown; (d) P-E anomaly averaged for the years 2170–2199 for RCP8.5-ice with different areas of the Atlantic; anomalies in regions of deep water formation of (e) salinity, (f) temperature, (g) potential density for RCP8.5-ice; (h)–(j) same as (e)–(g) but for RCP8.5.

Around the Year 2150, most of the sea ice in the Northern Hemisphere is gone in the RCP8.5 scenario and decreased to less than a half in the RCP4.5 scenario. No major differences between both models can be seen (Figures 1c and S2 in supporting information). The Nordic Seas, and, to a lesser extent, the Labrador Sea and the Irminger Sea show a positive salinity anomaly +0.5 to +1.0 psu (Figure 1 e,f). The increase in the RCP4.5 scenario is less pronounced than in the RCP8.5 scenario. Especially, the anomaly in the Labrador Sea is stronger in the setup with ISM than in the one without (Figures 1g and 1h). A freshening can be seen along the margin of Greenland, following the Labrador Current along the northern coast of Canada, and thus past regions of deep water formation (Figure 1d), following the streamlines in this area (Figures 1e–1h). This freshening is more pronounced in RCP4.5-ice than in RCP4.5 but only slightly stronger in RCP8.5-ice than in RCP8.5.

The temporal evolution of anomalies in temperature, salinity, and density for the regions of deep water formation in the North Atlantic (Figures 2e–2j) shows that salinity is decreasing initially at the surface (Figures 2e and 2h) but increasing in the subsurface. The effect of a subsurface increase in salinity that would result in an increase in potential density is overcompensated by strong warming of over 5 K (Figures 2f and 2i) from the surface to the depth. This leads to a decrease in potential density of up to −1.0 kg m $^{-3}$ at the

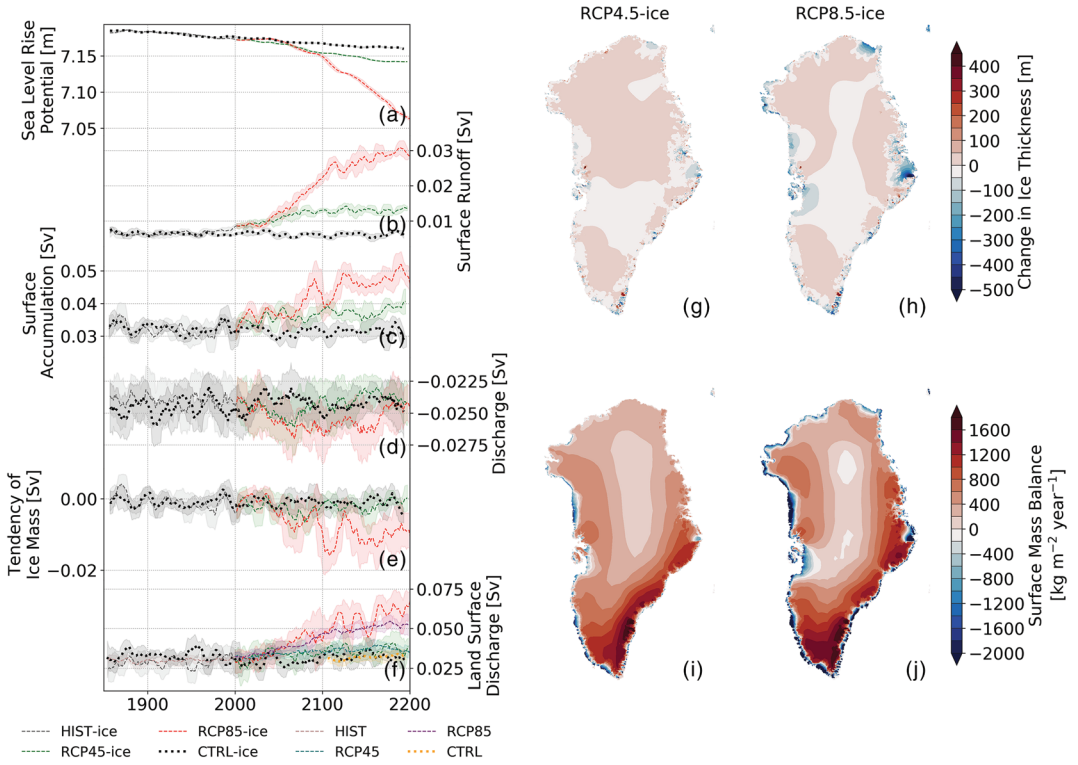

Figure 3. Time series of 11-year means and spatial changes of the GIS in the coupled simulations; shaded areas indicate 1 standard deviation. (a) The ice sheet's total volume expressed as sea-level rise potential, (b) surface runoff from the ISM, (c) surface accumulation, (d) discharge, (e) the ice sheet's total volume change, (f) surface runoff from the atmosphere model; for CTRL only the last 100 years are shown; (g and h) anomaly of the ice sheet's thickness for 2170–2199 for RCP4.5-ice and RCP8.5-ice, respectively; (i and j) the ice sheet's surface mass balance for 2170–2199 for RCP4.5-ice and RCP8.5-ice, respectively.

surface, eventuating in an enhanced stratification (Figures 2g and 2j). Thus, deep convection may be hampered, and the AMOC slows down. The negative surface salinity anomaly peaks around 2100 and decreases from then on (Figures 2e and 2h).

4. Feedback of the Greenland Ice Sheet

Overall the GIS is losing mass due to the increasing atmospheric temperatures. The total ice mass expressed as sea-level rise potential is decreasing from around 7.18 m to around 7.14 m in the RCP4.5 scenario and to around 7.06 m in the RCP8.5 scenario by the Year 2200, leading to a global sea-level rise of 0.04 and 0.12 m, respectively (Figure 3a).

The discharge contributes around 0.025 Sv to the ice mass loss and stays at a constant level throughout all simulations (Figure 3d). The surface runoff increases from less than 0.01 Sv in the control run to around 0.013 Sv in the RCP4.5-ice scenario and to over 0.03 Sv in the RCP8.5-ice scenario (Figure 3b). In contrast to that, the basal melting does contribute hardly anything to the ice mass loss (Figure S3 in the supporting information). These numbers add up to a total ablation of around 0.04 Sv for RCP4.5-ice and 0.06 Sv for RCP8.5-ice. The actual ice mass change shows a decal variability up to 0.015 Sv for RCP8.5-ice and is smaller for RCP4.5-ice (Figure 3e). The difference between total ablation and ice mass change is mainly due to local snow accumulation at the surface of the ice sheet (Figure 3c). Main areas are the southern and eastern parts of Greenland, whereas the western part is the main area of freshwater release (Figures 3i and 3j). The integrated surface accumulation increases from 0.032 to around 0.04 Sv in the RCP4.5-ice scenario and to around 0.05 Sv in the RCP8.5-ice scenario (Figure 3c) due to enhanced precipitation over Greenland (Figure 2d).

The additional precipitation that leads to local ice sheet growth in the model with ISM is released to the ocean immediately via river routing in the model without ISM. Thus, only the net ice mass change is added to the surface runoff of the land surface model. Due to the increased variability, there are intervals in which

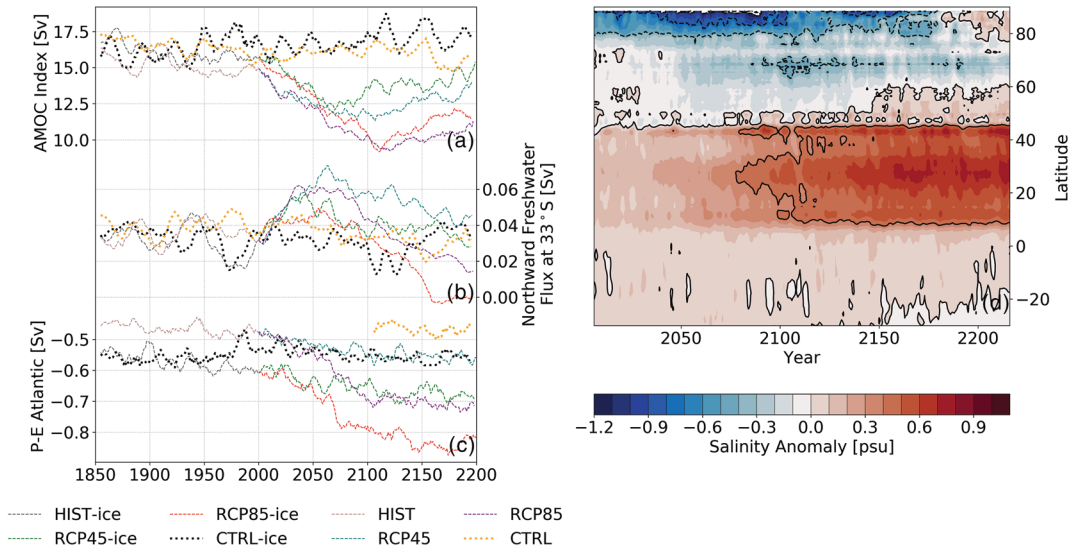

Figure 4. Time series of 11-year mean of (a) AMOC Index, defined as the streamfunction maximum between depths of 200 and 2,000 m and 30–60°N, (b) index for northward freshwater flux over 33°S, approximated after Vries and Weber (2005), (c) P-E integrated over Atlantic catchment area (Figure 2d); for CTRL only the last 100 years are shown for P-E Atlantic; (d) temporal evolution of salinity anomalies averaged over the upper 1,000 m of the Atlantic basin (Figure 2d) in RCP85-ice.

the coupled model runoff is smaller than the uncoupled one. However, the averaged land surface discharge into the North Atlantic by Greenland is around 0.01 Sv higher in RCP8.5-ice than in RCP8.5 and around the same for RCP4.5-ice and RCP4.5 (Figure 3f).

5. Multicentennial Trend of the AMOC

In this paper, the AMOC index is defined as the maximum of the meridional stream function between 200 and 2,000 m and 30–60°N. The AMOC shows a slowdown in all experiments. The AMOC index in the coupled model simulations is around 1 Sv higher than in the uncoupled model runs (Figure 4a). This corresponds to the slightly colder and more saline surface waters in the regions of deep water formation. The minimum AMOC index is reached around the Year 2075 for the RCP4.5 scenario and around the Year 2110 for the RCP8.5 scenario. Although the North Atlantic stays more stratified in the future scenarios compared to the control state, the AMOC recovers in all simulations.

The net freshwater export via the atmosphere is significantly larger than that via the ocean, changing from about −0.45 and −0.55 Sv in the control states to between −0.7 and −0.8 Sv for the RCP8.5 scenario in the uncoupled and coupled model setup, respectively (Figure 4c). This change overcompensates the decrease of oceanic freshwater import into the Atlantic (Figure 4b) and leads to an increase in ocean salinity, as also found by Lohmann (2003) and Latif et al. (2000). This result is supported by the fact that the highest increase in salinity can be seen at around 40°N, spreading northward (Figure 4d). While the North Atlantic shows a net atmospheric freshwater import (Figure 2a), this is overcompensated by the net loss over the Central and South Atlantic (Figure 2b and 2c). Figure 4d shows an initial increase in salinity between 0°N and 40°N, as suggested by Figure 2d. These are the areas of the highest P-E decrease. While there is an initial freshening between 40°N and 80°N, it turns into a positive salinity anomaly from the Year 2100 onward. This corresponds well with the AMOC slowdown and the decline in sea ice (Figure 1c), as there is no sea ice anymore that could act as a southward carrier of fresh water from the polar region.

6. Discussion

Our results show a net ice mass loss of the GIS in the future RCP8.5 scenario and, to a lesser extent, in the RCP4.5 scenario. While the land surface model captures the surface runoff, other mechanisms like the melt elevation feedback or basal melting and iceberg discharge are missing. Here, we show that the total ablation of the GIS is increased by around 0.01 Sv for the RCP8.5 scenario by including a dynamic ice sheet

model into our climate model. However, this additional 0.01 Sv is rather small compared to around 0.025 Sv of discharge alone. Due to our coupling mechanism, the absolute freshwater release is balanced out to some extent by local snow accumulation. Therefore, the signals in the tendency of ice mass and the land surface discharge are opposite, meaning that the GIS surface mass balance is potentially buffering the bare surface runoff of the land surface model. However, the strong decadal variability in the GIS mass balance is not seen for the AMOC. There is an interval between 2006 and around 2020, where the land surface discharge of RCP8.5-ice is lower than that of RCP8.5, corresponding to the positive GIS mass balance in this interval. However, the differences are relatively small and lay within the standard deviation of the time series. The amounts of freshwater released to the ocean of around 0.04 Sv in the RCP4.5-ice and around 0.06 Sv in the RCP8.5-ice (Figure 3f) are in accordance with the results from Lenaerts et al. (2015). As the surface runoff, discharge, and basal melting are treated equally, and all accounted as surface runoff, all melt-induced freshwater is released into the ocean directly. Therefore, no effects of iceberg transport are captured.

While the AMOC is around 1 Sv stronger in the coupled results than in the uncoupled ones, this seems to be due to a different initial state caused by coupling the ice sheet into the model. The overall trends of the AMOC are similar for both models: A decrease throughout the 21st century by around 7.5 Sv and a recovery starting at the beginning of the 22nd century. The total freshwater release of around 0.06 Sv brought into the ocean by the GIS in the coupled model setup is not sufficient to keep the AMOC in a weak state. This result is in contrast to the findings of Vizcano et al. (2008) and Mikolajewicz et al. (2007), who found freshwater perturbations of 0.02–0.03 Sv to be sufficient for preventing a recovery. Studies by Golledge et al. (2019) found a recovery of the AMOC in a simulation run without ice sheet feedbacks for the RCP8.5 scenario. However, although these studies did include dynamic ice sheet models, they used coarser ocean grids, not able to depict North Atlantic ocean currents like they can be seen in our results (Figures 1e–1h). Our results suggest that at least a share of the GIS meltwater is transported away by the Labrador Current (Figures 1e–1h), as the hot spot of freshwater release is located in West Greenland. These results may confirm the findings by Eden and Böning (2002) and Schmidt and Send (2007) that there is only little exchange between the Labrador Current and the Labrador Sea. While the increase in ocean temperature seems to be the main driver for the AMOC slowdown, as is also suggested by Swingedouw et al. (2015) and Kelly et al. (2016), the recovery appears to be driven by an increase in ocean salinity (Figures 2e–2j). Though the little effect, it seems essential to include a dynamic ice sheet model for appropriately depicting the places of freshwater release.

Different authors argue that a positive Atlantic freshwater import constitutes a negative feedback for the AMOC, leading to a recovery of the AMOC after an initial perturbation (Jackson, 2013; Liu et al., 2013; Rahmstorf, 1996). This is in accordance with our results (Figure 4b). The changes in the Atlantic freshwater import are little compared to the changes in P-E over the southern and central Atlantic (Figure 2) that seem to be the main contributor of the Atlantic salinity increase. The positive salinity anomaly in the North Atlantic follows a trend observed since the 1950s (Stocker et al., 2013), which continues in our experiments. Studies by Lind et al. (2018) show that Barents Sea warming, observed since 1970, can be linked to a decrease in Arctic sea ice, resulting in enhanced evaporation and to an Atlantic-dominated regime. The negative anomalies in P-E in the Baffin Bay, the Barents Sea, and the Kara Sea support this result (Figure 2d). However, the strongest salinity anomalies occur at around 40°N and seem to spread northward (Figure 4d). The near-surface freshening may be the result of the AMOC weakening. The following positive salinity anomaly around 80°N may be the result of a reduction in sea ice transport from the polar region, as also seen in other studies by W. Liu, Fedorov, et al. (2019).

7. Conclusion

In our newly developed coupled climate-ice sheet model AWI-ESM, we simulate the climate warming scenarios, to assess the effects of melt-induced fresh water on AMOC. Our oceanic multiscale model allows us to resolve ocean boundary currents and regions of deep-water formation. Our model shows an AMOC recovery for the RCP8.5 scenario (with fixed CO_2 forcing from 2100 onward) starting at the beginning of the 22nd century onward, for both versions with and without a dynamic ISM. The differences in the experiments are relatively minor. Also, the total freshwater release from the Greenland ice sheet is similar for both versions. However, the interactive ISM adds pronounced decadal variability to the surface runoff into the North Atlantic, resulting in intervals, where the surface accumulation overcompensates the ice sheet melting. This feature is not present in conventional climate models, as they lack ice sheet dynamics.

Our results also suggest that the atmospheric freshwater transport by enhanced evaporation in the Atlantic realm plays a major role in an AMOC recovery. The net increase in evaporation over the central and southern Atlantic is stronger than the increase in precipitation in the North Atlantic.

As a logical next step, we will investigate the role of the Labrador Current on the GIS melt-induced freshening of the North Atlantic. Since iceberg discharge can make up a large portion of total ice sheet mass loss, the incorporation of an iceberg model is useful. Such a model would enable for simulating the freshwater release by calving, without the compensating effect of the total GIS mass balance. Including iceberg calving and transport would allow salinity changes to occur directly over deep water formation sites, thereby enabling a more realistic representation of the freshwater dynamics in the North Atlantic. In the Southern Ocean, an iceberg model would allow for simulating the disintegration of Antarctic ice shelves (Pollard & DeConto, 2009; Sutter et al., 2016; Timmermann & Hellmer, 2013).

Data Availability Statements

Code for the AWI-ESM-PISM coupler `SCOPE` is available under https://gitlab.awi.de/pgierz/scope (Gierz et al., 2020) and can also be installed via the Python package managing system, `pip`, via the command `pip install scope-coupler`. `SCOPE` is a free software, licensed under the GNU Public License, v.3. The Parallel Ice Sheet Model `PISM` is available from this site (https://github.com/pism/pism). `FESOM` is also a free software and available from this site (https://github.com/fesom/fesom). `ECHAM6`, which is the atmosphere model of the `MPI-ESM`, is a property of the Max Planck Institute for Meteorology. Its model code is available at https://code.mpimet.mpg.de/login?back_url=https%3A%2F%2Fcode.mpimet.mpg.de%2Fprojects%2Fmpi-esm-users%2Ffiles after registration at this site (https://www.mpimet.mpg.de/en/science/models/availability-licenses). For further information, please contact karl-hermann.wieners@mpimet.mpg.de. Modifications required to reconstruct the version of `ECHAM6` in the `AWI-ESM` are avaiable as patch file from this site (https://gitlab.awi.de/pgierz/echam6-patch). Simulation output is provided via PANGAEA (https://doi.org/10.1594/PANGAEA.916162).

Acknowledgments
Thanks go to the Max-Planck Institute in Hamburg (Germany), the University of Alaska Fairbanks (USA), the Potsdam Institute for Climate Impact Research, and colleagues from the Alfred-Wegener Institute for making ECHAM6-JSBACH and FESOM, AWI-ESM, PISM available to us. We also thank the two anonymous reviewers for their constructive suggestions. We acknowledge financial support from PACES and REKLIM through the Helmholtz association, as well as from the BMBF projects PalMOD, PACMEDY, and NOPAWAC. Computational resources were made available by the infrastructure and support of the computing center of the Alfred Wegener Institute in Bremerhaven and the DKRZ in Hamburg, Germany. L. A. and C. D. were funded by the Federal Ministry of Education and Research initiative PalMod: Kopplung des AWI EisschildModells mit dem Klimamodell ECHAM/MPIOM; Grant 01LP1502B (Project PalMod1.1). P. G. is funded by the Federal Ministry for Education and Research initiative PalMod: Simulating a Full Glacial Cycle; BMBF Grant 01LP1503B (Project PalMod1.2). G. L. acknowledges funding via the Alfred Wegener Institute's research programme PACES2.

References

Barker, S., Diz, P., Vautravers, M. J., Pike, J., Knorr, G., Hall, I. R., & Broecker, W. S. (2009). Interhemispheric Atlantic seesaw response during the last deglaciation. *Nature*, *457*(7233), 1097–1102. https://doi.org/10.1038/nature07770

Barker, S., Knorr, G., Vautravers, M. J., Diz, P., & Skinner, L. C. (2010). Extreme deepening of the Atlantic overturning circulation during deglaciation. *Nature Geoscience*, *3*(8), 567–571. https://doi.org/10.1038/ngeo921

Bianchi, G. G., & McCave, I. N. (1999). Holocene periodicity in North Atlantic climate and deep-ocean flow south of Iceland. *Nature*, *397*(6719), 515–517. https://doi.org/10.1038/17362

Böning, C. W., Behrens, E., Biastoch, A., Getzlaff, K., & Bamber, J. L. (2016). Emerging impact of Greenland meltwater on deepwater formation in the North Atlantic ocean. *Nature Geoscience*, *9*(7), 523–527. https://doi.org/10.1038/ngeo2740

Broecker, W. S. (1990). Salinity history of the northern Atlantic during the last deglaciation. *Paleoceanography*, *5*(4), 459–467. https://doi.org/10.1029/PA005i004p00459

Broecker, W. S. (2000). Was a change in thermohaline circulation responsible for the little ice age? *Proceedings of the National Academy of Sciences*, *97*(4), 1339–1342. https://doi.org/10.1073/pnas.97.4.1339

Broecker, W. S., Andree, M., Wolfli, W., Oeschger, H., Bonani, G., Kennett, J., & Peteet, D. (1988). The chronology of the last Deglaciation: Implications to the cause of the Younger Dryas event. *Paleoceanography*, *3*(1), 1–19. https://doi.org/10.1029/PA003i001p00001

Broecker, W. S., Peteet, D. M., & Rind, D. (1985). Does the ocean atmosphere system have more than one stable mode of operation? *Nature*, *315*(6014), 21–26. https://doi.org/10.1038/315021a0

Bryan, F. (1986). High-latitude salinity effects and interhemispheric thermohaline circulations. *Nature*, *323*(6086), 301–304. https://doi.org/10.1038/323301a0

Clark, P. U., Pisias, N. G., Stocker, T. F., & Weaver, A. J. (2002). The role of the thermohaline circulation in abrupt climate change. *Nature*, *415*(6874), 863–869. https://doi.org/10.1038/415863a

Clarke, L., Edmonds, J., Jacoby, H., Pitcher, H., Reilly, J., & Richels, R. (2007). Scenarios of greenhouse gas emissions and atmospheric concentrations. Department of Energy, Office of Biological & Environmental Research, 166.

Danek, C., Scholz, P., & Lohmann, G. (2019). Effects of high resolution and spinup time on modeled North Atlantic circulation. *Journal of Physical Oceanography*, *49*(5), 1159–1181. https://doi.org/10.1175/JPO-D-18-0141.1

Dima, M., & Lohmann, G. (2010). Evidence for two distinct modes of large-scale ocean circulation changes over the last century. *Journal of Climate*, *23*(1), 5–16. https://doi.org/10.1175/2009JCLI2867.1

Driesschaert, E., Fichefet, T., Goosse, H., Huybrechts, P., Janssens, I., Mouchet, A., et al. (2007). Modeling the influence of Greenland ice sheet melting on the Atlantic Meridional Overturning Circulation during the next millennia. *Geophysical Research Letters*, *34*, L10707. https://doi.org/10.1029/2007GL029516

Eden, C., & Böning, C. (2002). Sources of eddy kinetic energy in the Labrador Sea. *Journal of Physical Oceanography*, *32*(12), 3346–3363. https://doi.org/10.1175/1520-0485(2002)032<3346:SOEKEI>2.0.CO;2

Gierz, P., Ackermann, L., Rodehacke, C., Krebs-Kanzow, U., Stepanek, C., Barbi, D., & Lohmann, G. (2020). Simulating interactive ice sheets in the multi-resolution AWI-ESM 1.2: A case study using scope 1.0. Geoscientific Model Development.

Gierz, P., Lohmann, G., & Wei, W. (2015). Response of Atlantic overturning to future warming in a coupled atmosphere-ocean-ice sheet model: Response of AMOC in a coupled GCM-ISM. *Geophysical Research Letters*, *42*, 6811–6818. https://doi.org/10.1002/2015GL065276

Golledge, N. R., Keller, E. D., Gomez, N., Naughten, K. A., Bernales, J., Trusel, L. D., & Edwards, T. L. (2019). Global environmental consequences of twenty-first-century ice-sheet melt. *Nature*, *566*(7742), 65. https://doi.org/10.1038/s41586-019-0889-9

Hagemann, S., & Dümenil, L. (1997). A parametrization of the lateral waterflow for the global scale. *Climate Dynamics*, *14*(1), 17–31. https://doi.org/10.1007/s003820050205

Hagemann, S., & Gates, L. D. (2003). Improving a subgrid runoff parameterization scheme for climate models by the use of high resolution data derived from satellite observations. *Climate Dynamics*, *21*(3-4), 349–359.

Hu, A., Meehl, G. A., Han, W., & Yin, J. (2009). Transient response of the moc and climate to potential melting of the Greenland ice sheet in the 21st century. *Geophysical Research Letters*, *36*, L10707. https://doi.org/10.1029/2009GL037998

Hu, A., Meehl, G. A., Han, W., & Yin, J. (2011). Effect of the potential melting of the Greenland ice sheet on the Meridional Overturning Circulation and global climate in the future. *Deep Sea Research Part II: Topical Studies in Oceanography*, *58*(17), 1914–1926. https://doi.org/10.1016/j.dsr2.2010.10.069

Jackson, L. C. (2013). Shutdown and recovery of the AMOC in a coupled global climate model: The role of the advective feedback. *Geophysical Research Letters*, *40*, 1182–1188. https://doi.org/10.1002/grl.50289

Jungclaus, J. H., Haak, H., Esch, M., Roeckner, E., & Marotzke, J. (2006). Will Greenland melting halt the thermohaline circulation? *Geophysical Research Letters*, *33*, L17708. https://doi.org/10.1029/2006GL026815

Keigwin, L. D., Jones, G. A., Lehman, S. J., & Boyle, E. A. (1991). Deglacial meltwater discharge, North Atlantic Deep Circulation, and abrupt climate change. *Journal of Geophysical Research*, *96*(C9), 16,811–16,826. https://doi.org/10.1029/91JC01624

Kelly, K. A., Drushka, K., Thompson, L., Bars, D. L., & McDonagh, E. L. (2016). Impact of slowdown of Atlantic overturning circulation on heat and freshwater transports. *Geophysical Research Letters*, *43*, 7625–7631. https://doi.org/10.1002/2016GL069789

Knorr, G., & Lohmann, G. (2007). Rapid transitions in the Atlantic thermohaline circulation triggered by global warming and meltwater during the last deglaciation. *Geochemistry, Geophysics, Geosystems*, *8*, Q12006. https://doi.org/10.1029/2007GC001604

Latif, M., Roeckner, E., Mikolajewicz, U., & Voss, R. (2000). Tropical stabilization of the thermohaline circulation in a Greenhouse warming simulation. *Journal of Climate*, *13*(11), 1809–1813. https://doi.org/10.1175/1520-0442(2000)013<1809:L>2.0.CO;2

Lenaerts, J. T. M., Bars, D. L., Kampenhout, L., Vizcaino, M., Enderlin, E. M., & Broeke, M. R. (2015). Representing Greenland ice sheet freshwater fluxes in climate models. *Geophysical Research Letters*, *42*, 6373–6381. https://doi.org/10.1002/2015GL064738

Lind, S., Ingvaldsen, R. B., & Furevik, T. (2018). Arctic warming hotspot in the northern Barents Sea linked to declining sea-ice import. *Nature Climate Change*, *8*(7), 634–639. https://doi.org/10.1038/s41558-018-0205-y

Liu, W., Fedorov, A., & Svellec, F. (2019). The mechanisms of the Atlantic Meridional Overturning Circulation slowdown induced by Arctic sea ice decline. *Journal of Climate*, *32*(4), 977–996. https://doi.org/10.1175/JCLI-D-18-0231.1

Liu, Y., Hallberg, R., Sergienko, O., Samuels, B. L., Harrison, M., & Oppenheimer, M. (2018). Climate response to the meltwater runoff from Greenland ice sheet: Evolving sensitivity to discharging locations. *Climate Dynamics*, *51*(5-6), 1733–1751. https://doi.org/10.1007/s00382-017-3980-7

Liu, W., Liu, Z., & Hu, A. (2013). The stability of an evolving Atlantic meridional overturning circulation. *Geophysical Research Letters*, *40*, 1562–1568. https://doi.org/10.1002/grl.50365

Lohmann, G. (2003). Atmospheric and oceanic freshwater transport during weak Atlantic overturning circulation. *Tellus A: Dynamic Meteorology and Oceanography*, *55*(5), 438–449. https://doi.org/10.3402/tellusa.v55i5.12108

Manabe, S., & Stouffer, R. J. (1995). Simulation of abrupt climate change induced by freshwater input to the North Atlantic Ocean. *Nature*, *378*(6553), 165–167. https://doi.org/10.1038/378165a0

Martin, M. A., Winkelmann, R., Haseloff, M., Albrecht, T., Bueler, E., Khroulev, C., & Levermann, A. (2011). The Potsdam parallel ice sheet model (PISM-PIK) Part 2: Dynamic equilibrium simulation of the Antarctic ice sheet. *The Cryosphere*, *5*(3), 727–740. https://doi.org/10.5194/tc-5-727-2011

McManus, J. F., Francois, R., Gherardi, J.-M., Keigwin, L. D., & Brown-Leger, S. (2004). Collapse and rapid resumption of atlantic meridional circulation linked to deglacial climate changes. *Nature*, *428*(6985), 834–837. https://doi.org/10.1038/nature02494

Mikolajewicz, U., Vizcano, M., Jungclaus, J., & Schurgers, G. (2007). Effect of ice sheet interactions in anthropogenic climate change simulations. *Geophysical Research Letters*, *34*, L18706. https://doi.org/10.1029/2007GL031173

Pollard, D., & DeConto, R. M. (2009). Modelling West Antarctic ice sheet growth and collapse through the past five million years. *Nature*, *458*(7236), 329–332.

Rackow, T., Goessling, H. F., Jung, T., Sidorenko, D., Semmler, T., Barbi, D., & Handorf, D. (2018). Towards multi-resolution global climate modeling with ECHAM6-FESOM. Part II: Climate variability. *Climate Dynamics*, *50*(7-8), 2369–2394. https://doi.org/10.1007/s00382-016-3192-6

Rahmstorf, S. (1996). On the freshwater forcing and transport of the Atlantic thermohaline circulation:. *Climate Dynamics*, *12*(12), 799–811. https://doi.org/10.1007/s003820050144

Rahmstorf, S. (2002). Ocean circulation and climate during the past 120,000 years. *Nature*, *419*, 207–214. https://doi.org/10.1038/nature01090

Reick, C. H., Raddatz, T., Brovkin, V., & Gayler, V. (2013). Representation of natural and anthropogenic land cover change in MPI-ESM. *Journal of Advances in Modeling Earth Systems*, *5*, 459–482. https://doi.org/10.1002/jame.20022

Riahi, K., Grübler, A., & Nakicenovic, N. (2007). Scenarios of long-term socio-economic and environmental development under climate stabilization. *Technological Forecasting and Social Change*, *74*(7), 887–935. https://doi.org/10.1016/j.techfore.2006.05.026

Schmidt, S., & Send, U. (2007). Origin and composition of seasonal Labrador Sea freshwater. *Journal of Physical Oceanography*, *37*(6), 1445–1454. https://doi.org/10.1175/JPO3065.1

Sidorenko, D., Rackow, T., Jung, T., Semmler, T., Barbi, D., Danilov, S., et al. (2015). Towards multi-resolution global climate modeling with ECHAM FESOM. Part I: Model formulation and mean climate. *Climate Dynamics*, *44*(3-4), 757–780. https://doi.org/10.1007/s00382-014-2290-6

Stammer, D., Agarwal, N., Herrmann, P., Köhl, A., & Mechoso, C. R. (2011). Response of a coupled ocean–atmosphere model to Greenland ice melting. *Surveys in geophysics*, *32*(4-5), 621.

Stevens, B., Giorgetta, M., Esch, M., Mauritsen, T., Crueger, T., Rast, S., et al. (2013). Atmospheric component of the MPI-M Earth system model: ECHAM6. *Journal of Advances in Modeling Earth Systems*, *5*, 146–172. https://doi.org/10.1002/jame.20015

Stocker, T. F., Qin, D., Plattner, G.-K., Tignor, M., Allen, S. K., Boschung, J., et al. (2013). Climate change 2013: The physical science basis. Contribution of working group I to the fifth assessment report of the intergovernmental panel on climate change, 1535.

Stocker, T. F., & Schmittner, A. (1997). Influence of CO_2 emission rates on the stability of the thermohaline circulation. *Nature*, *388*(6645), 862–865. https://doi.org/10.1038/42224

Sutter, J., Gierz, P., Grosfeld, K., Thoma, M., & Lohmann, G. (2016). Ocean temperature thresholds for last interglacial West Antarctic ice sheet collapse. *Geophysical Research Letters*, *43*, 2675–2682. https://doi.org/10.1002/2016GL067818

Swingedouw, D., & Braconnot, P. (2007). Effect of the Greenland ice-sheet melting on the response and stability of the AMOC in the next centuries. In A. Schmittner, J. C. H. Chiang, & S. R. Hemming (Eds.), *Geophysical Monograph Series* (Vol. 173, pp. 383–392). Washington, D. C.: American Geophysical Union.

Swingedouw, D., Rodehacke, C. B., Olsen, S. M., Menary, M., Gao, Y., Mikolajewicz, U., & Mignot, J. (2015). On the reduced sensitivity of the Atlantic overturning to Greenland ice sheet melting in projections: A multi-model assessment. *Climate Dynamics*, *44*(11-12), 3261–3279. https://doi.org/10.1007/s00382-014-2270-x

Thibodeau, B., Not, C., Zhu, J., Schmittner, A., Noone, D., Tabor, C., et al. (2018). Last century warming over the Canadian Atlantic shelves linked to weak Atlantic meridional overturning circulation. *Geophysical Research Letters*, *45*, 12,376–12,385. https://doi.org/10.1029/2018GL080083

Timmermann, R., & Hellmer, H. H. (2013). Southern Ocean warming and increased ice shelf basal melting in the twenty-first and twenty-second centuries based on coupled ice-ocean finite-element modelling. *Ocean Dynamics*, *63*(9-10), 1011–1026.

Vizcano, M., Mikolajewicz, U., Gröger, M., Maier-Reimer, E., Schurgers, G., & Winguth, A. M. E. (2008). Long-term ice sheet climate interactions under anthropogenic greenhouse forcing simulated with a complex Earth system model. *Climate Dynamics*, *31*(6), 665–690. https://doi.org/10.1007/s00382-008-0369-7

Vries, P., & Weber, S. L. (2005). The Atlantic freshwater budget as a diagnostic for the existence of a stable shut down of the meridional overturning circulation. *Geophysical Research Letters*, *32*, L09606. https://doi.org/10.1029/2004GL021450

Wang, Q., Danilov, S., Sidorenko, D., Timmermann, R., Wekerle, C., Wang, X., et al. (2014). The finite element sea ice-ocean model (fesom) v.1.4: Formulation of an ocean general circulation model. *Geoscientific Model Development*, *7*(2), 663–693. https://doi.org/10.5194/gmd-7-663-2014

Wang, H., Legg, S., & Hallberg, R. (2018). The effect of arctic freshwater pathways on North Atlantic convection and the Atlantic meridional overturning circulation. *Journal of Climate*, *31*(13), 5165–5188. https://doi.org/10.1175/JCLI-D-17-0629.1

Weaver, A. J., Sedlek, J., Eby, M., Alexander, K., Crespin, E., Fichefet, T., et al. (2012). Stability of the Atlantic meridional overturning circulation: A model intercomparison. *Geophysical Research Letters*, *39*, L20709. https://doi.org/10.1029/2012GL053763

Weijer, W., Maltrud, M. E., Hecht, M. W., Dijkstra, H. A., & Kliphuis, M. A. (2012). Response of the Atlantic Ocean circulation to Greenland ice sheet melting in a strongly-eddying ocean model. *Geophysical Research Letters*, *39*, L09606. https://doi.org/10.1029/2012GL051611

Winkelmann, R., Martin, M. A., Haseloff, M., Albrecht, T., Bueler, E., Khroulev, C., & Levermann, A. (2011). The Potsdam parallel ice sheet model (PISM-PIK) Part 1: Model description. *The Cryosphere*, *5*(3), 715–726. https://doi.org/10.5194/tc-5-715-2011

Wise, M., Calvin, K., Thomson, A., Clarke, L., Bond-Lamberty, B., Sands, R., et al. (2009). Implications of limiting CO_2 concentrations for land use and energy. *Science*, *324*(5931), 1183–1186. https://doi.org/10.1126/science.1168475

Yang, Q., Dixon, T. H., Myers, P. G., Bonin, J., Chambers, D., van den Broeke, M. R., et al. (2016). Recent increases in Arctic freshwater flux affects Labrador Sea convection and Atlantic overturning circulation. *Nature Communications*, *7*(1), 10525. https://doi.org/10.1038/ncomms10525